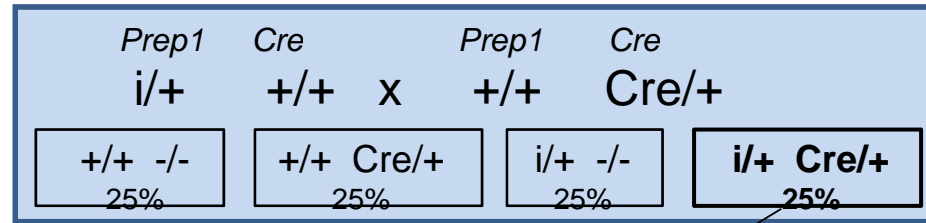
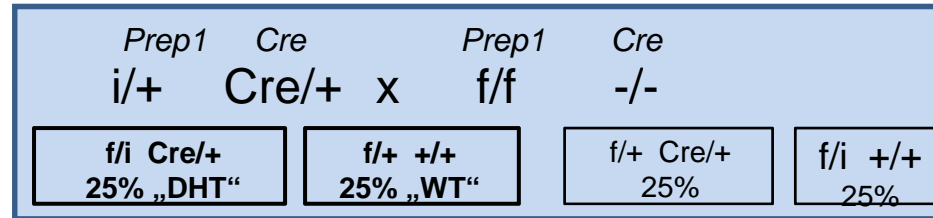


A

1) Transfer hypomorphic *Prep1* allele on MCK-Cre-line



2) Cross with *Prep1<sup>flox</sup>* mice



B

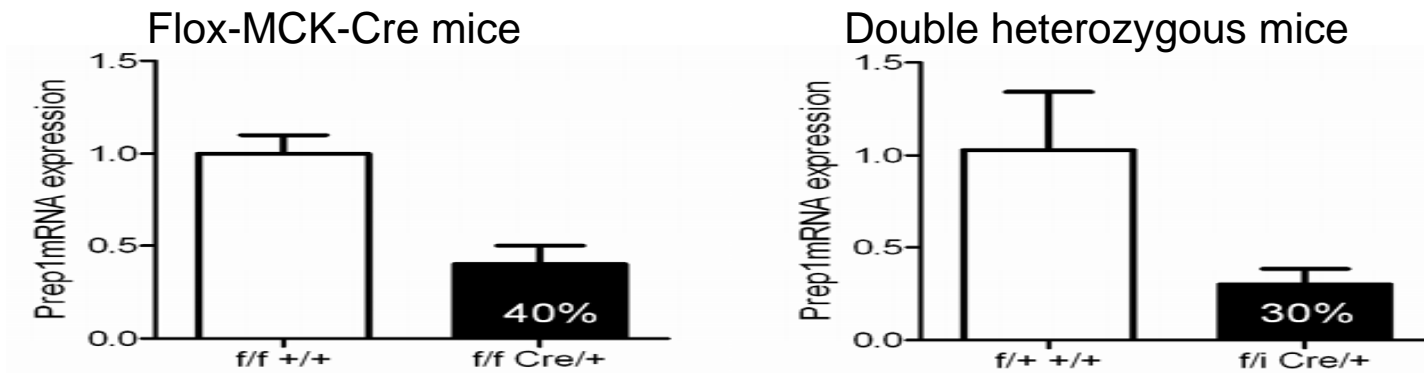


Figure 1: Breeding strategy of *Prep1* double heterozygous mice (A) (i=hypomorphic allele, f=floxed allele). Expression of *Prep1* in *Prep1*-flox-MCK-Cre and *Prep1* double heterozygous mice (B)

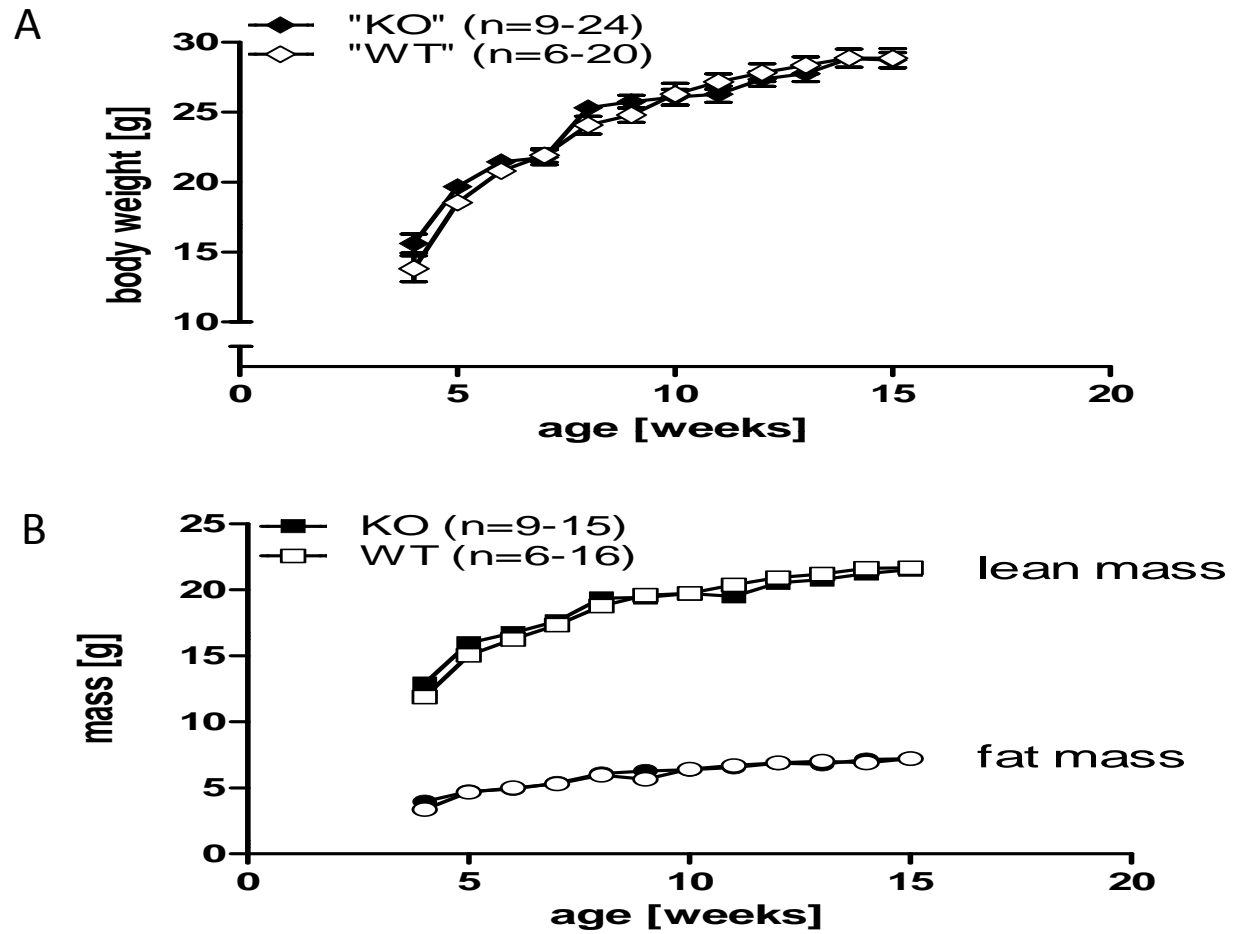
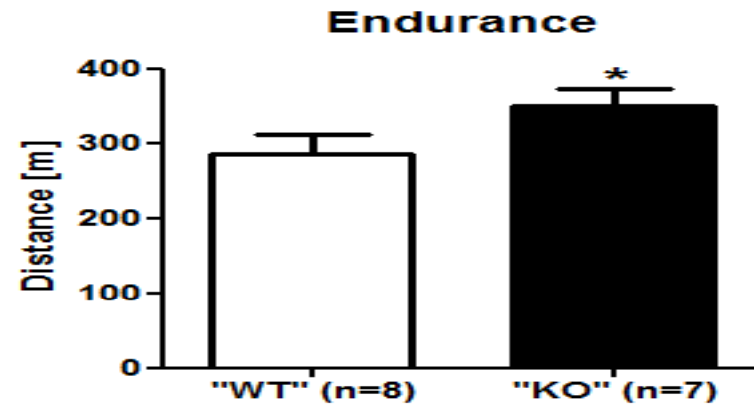


Figure 2: Body mass (A) and body composition (B) of double heterozygous (KO) and wild-type (WT) mice.

A



B

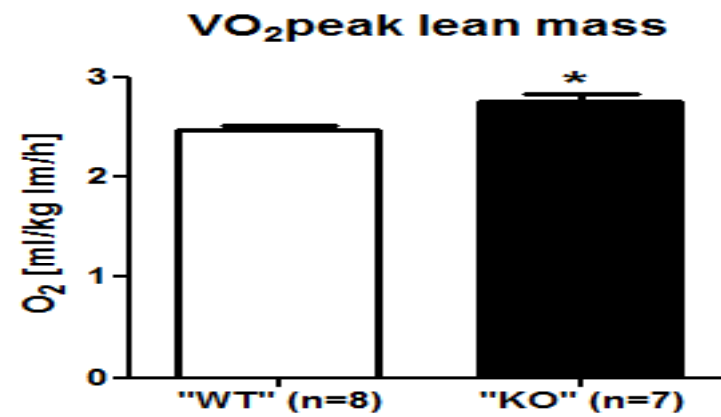


Figure 3: (A) Maximal running distance and (B) oxidative capacity (VO<sub>2</sub>peak) of double heterozygous („KO“) and wildtype („WT“) mice. Statistical significance was calculated with students t-test (p<0.05).

## Effect of Prep1 in 3T3L1 pre-adipocytes and adipocytes

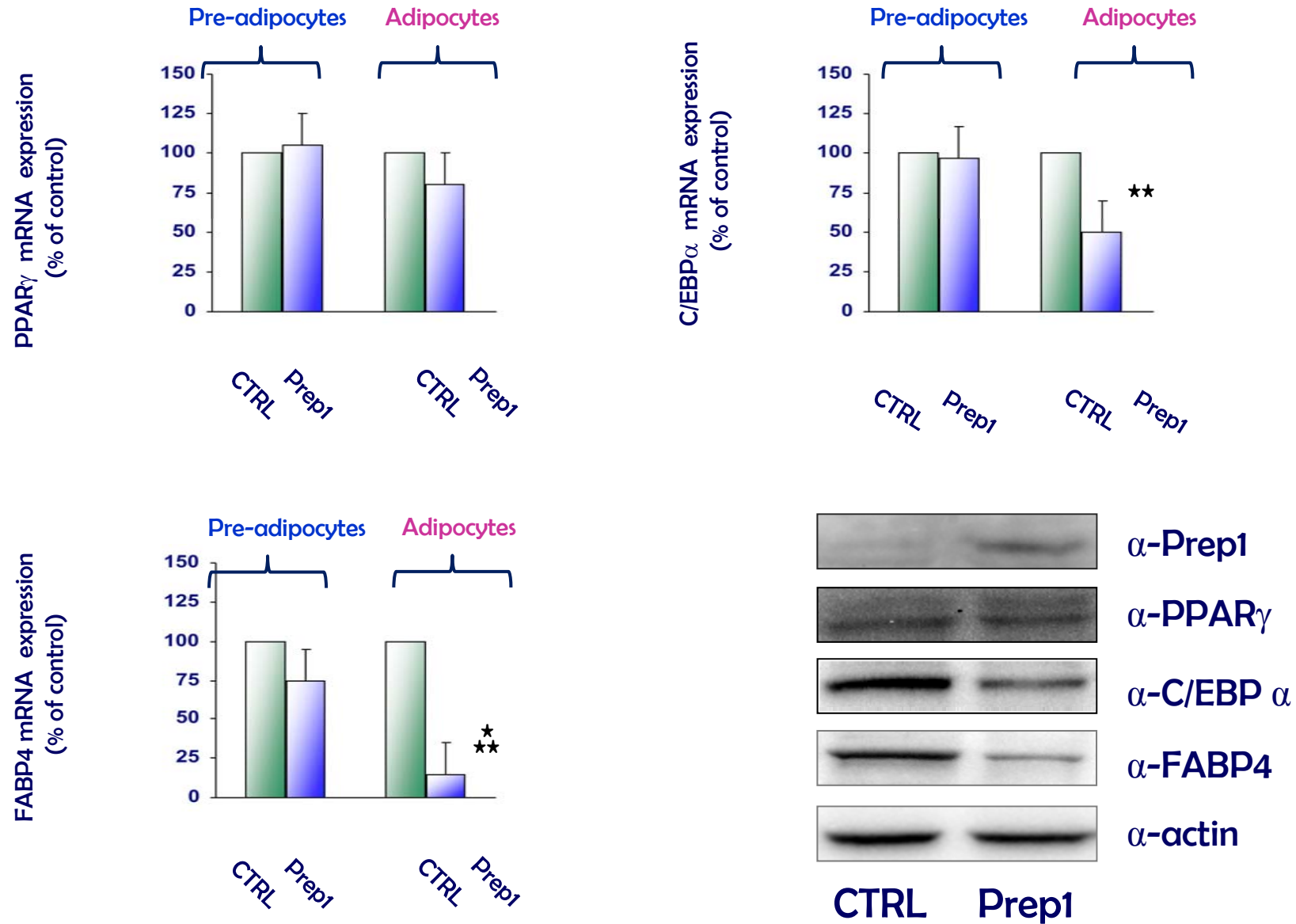


Figure 4

FIG.2 - C/EBP $\alpha$ , FABP4 and PPAR $\gamma$  expression in adipose tissue from *prep1*<sup>i/+</sup> mice

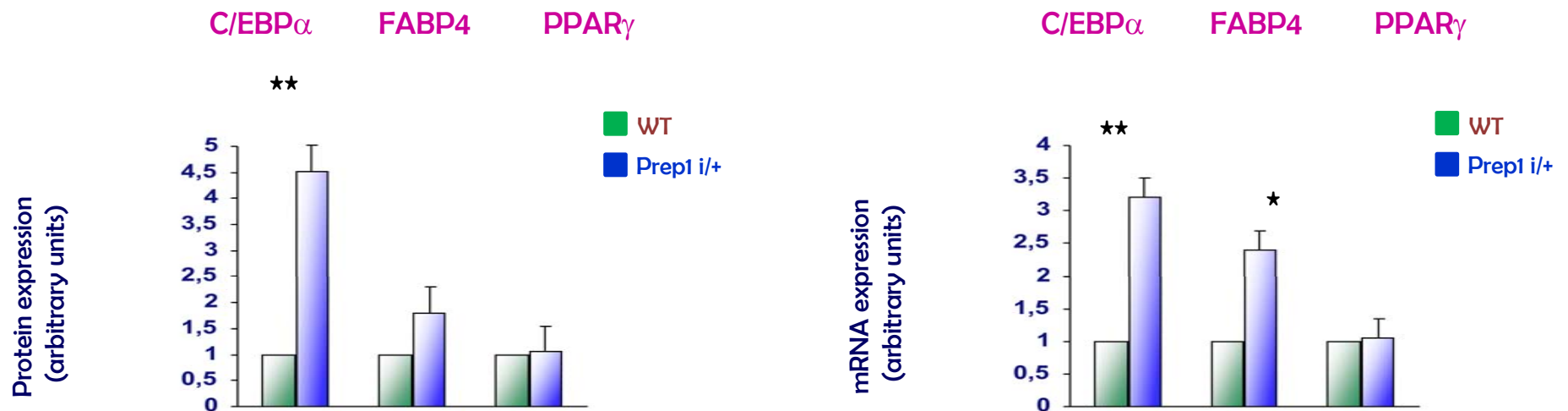
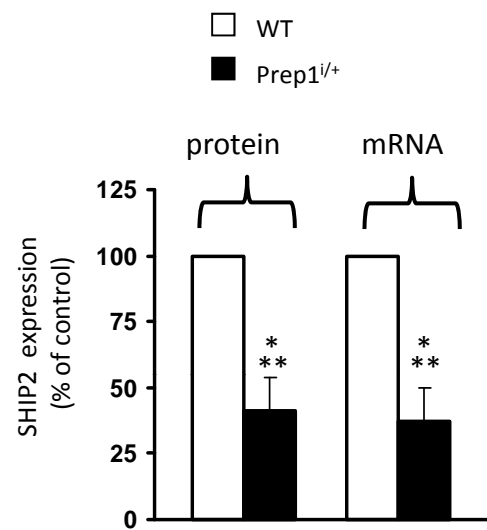
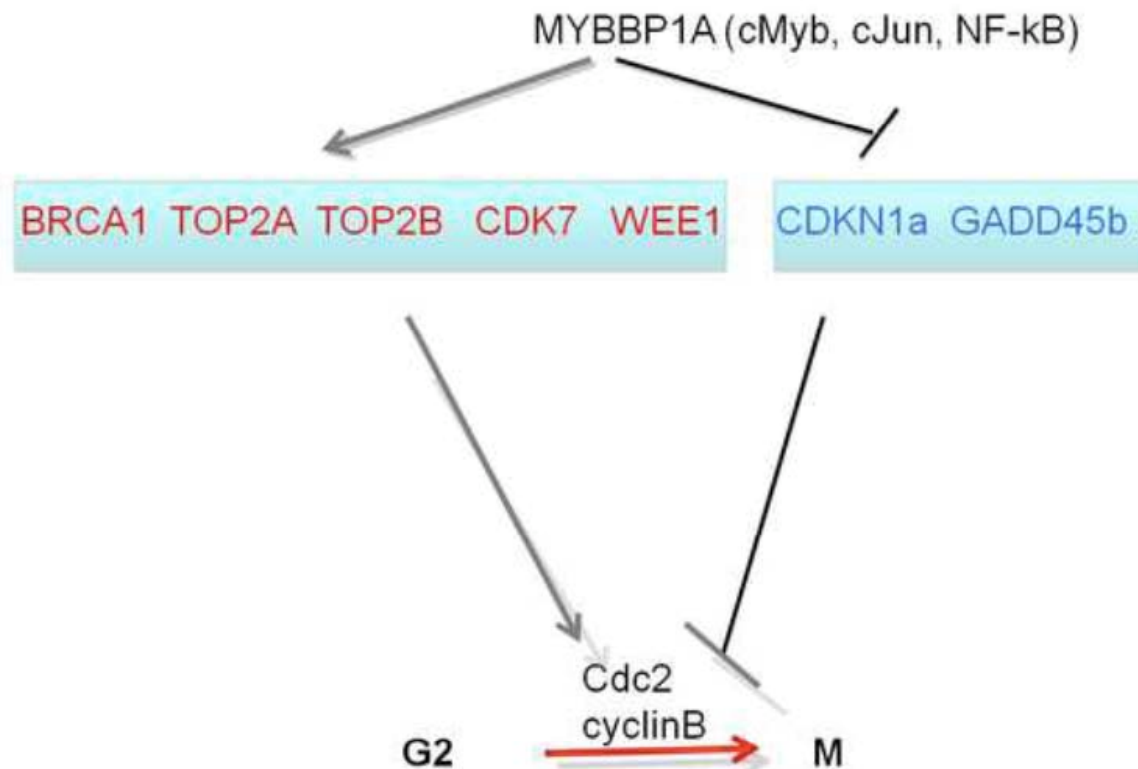


Figure 5: Expression of c/EBP $\alpha$ , FABP4 and PPAR $\gamma$  in wild type and Prep1<sup>i/+</sup> mice Measured by immunoblotting (left) and qPCR (right).



**Fig.6** SHIP2 expression in liver from wt and prep1i/+ mice



**Figure 7: Role of p160 Mybbp1a in cell cycle genes.** The figure depicts the connection between MYBBP1A, the genes regulating the cell cycle that are altered by MYBBP1A down-regulation and their function. In particular, the expression of red genes is increased in the absence of MYBBP1A, while those in blue are decreased.

Thus, MYBBP1A induces the inhibitors of Cdc2/cyclinB and down-regulates those that activate. Note that although the figure focuses on the G2/M phase, some of the genes function also at the G1/S (in particular CDKN1A). MYBBP1A might act by regulating the synthesis and/or activity of one or more of its partner transcription factors (cMyb, cJun, NF-kB, Prep1). In fact, the level of cJun mRNA is increased upon MYBBP1A down-regulation.

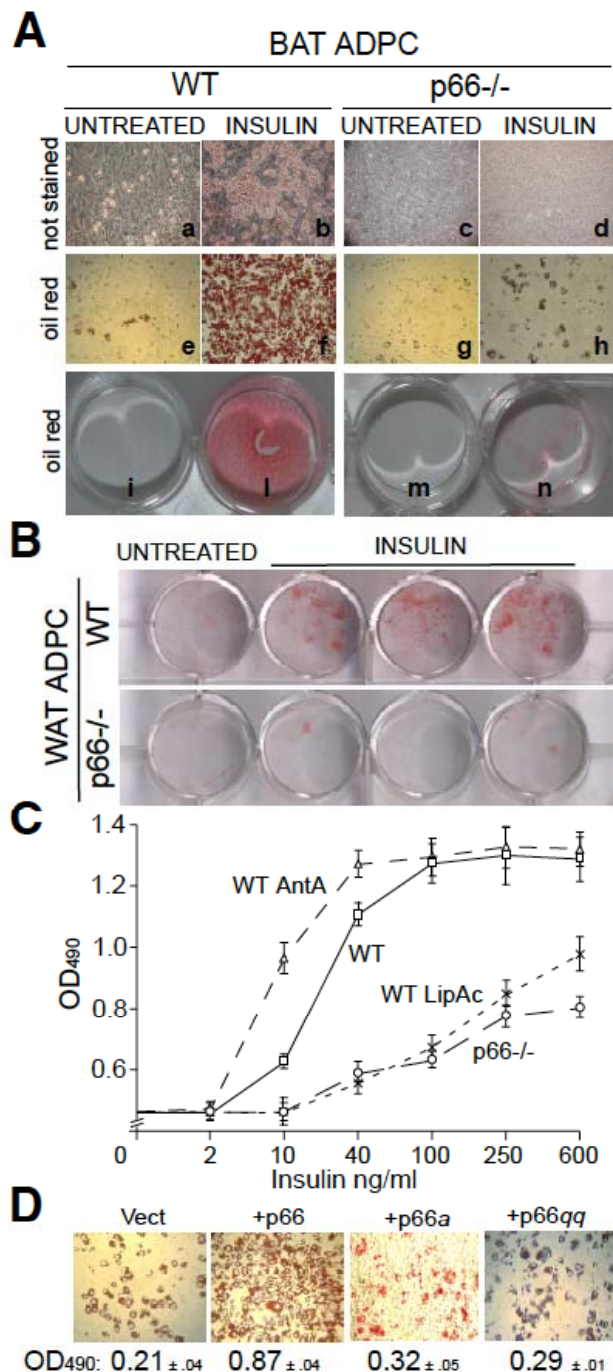


**Figure 8.** *P66<sup>Shc</sup> regulation of insulin-induced triglyceride accumulation.*

White light microscopy pictures (a-h) and plate micrographs (i-n) of unstained (a-d) and Oil red stained (e-h, i-n) BAT adipocytes from WT and p66<sup>Shc</sup><sup>-/-</sup> mice. Cells were left untreated (a, e, c, g, i, m) or treated with insulin for 6 days (b, f, d, h, j and n). **B.** Micrographs of plates of Oil red-stained of WT and p66<sup>Shc</sup><sup>-/-</sup> WAT adipocytes, untreated and after insulin treatment. **C.** OD values of Oil red extracts from stained WT, antimycin A (AntA)- or lipoic acid (LipAc)- treated WT and p66<sup>Shc</sup><sup>-/-</sup> BAT adipocytes (average of 8 independent experiments for each condition). **D.** White light microscopy pictures of Oil red-stained p66<sup>Shc</sup><sup>-/-</sup> BAT adipocytes infected with empty (Vect), p66<sup>Shc</sup>, p66<sup>Shc</sup>a or p66<sup>Shc</sup>qq retroviruses and treated with insulin, and their corresponding optical density (OD; 490nm) values.



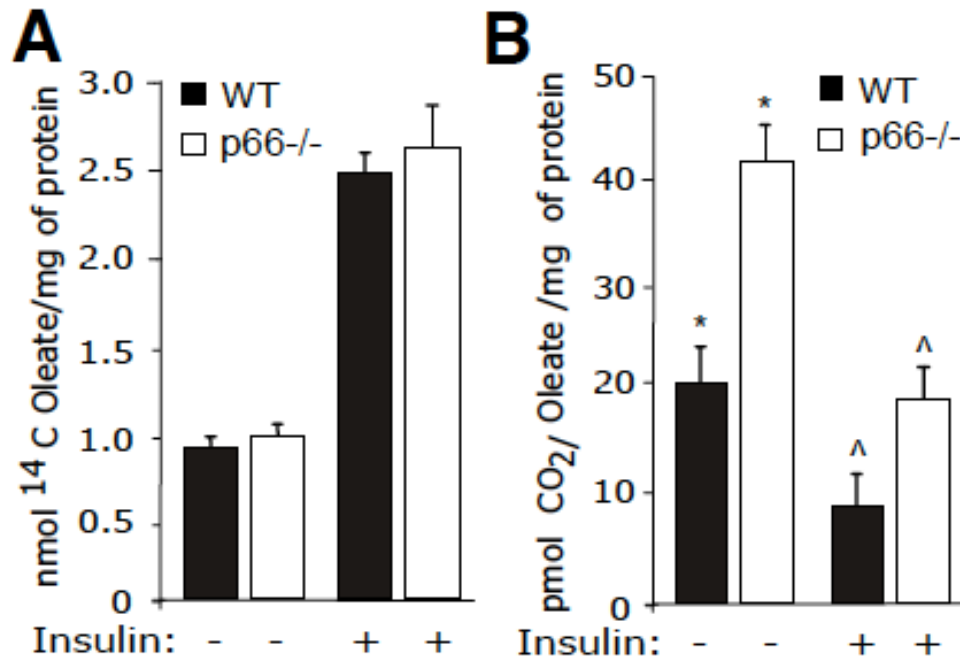
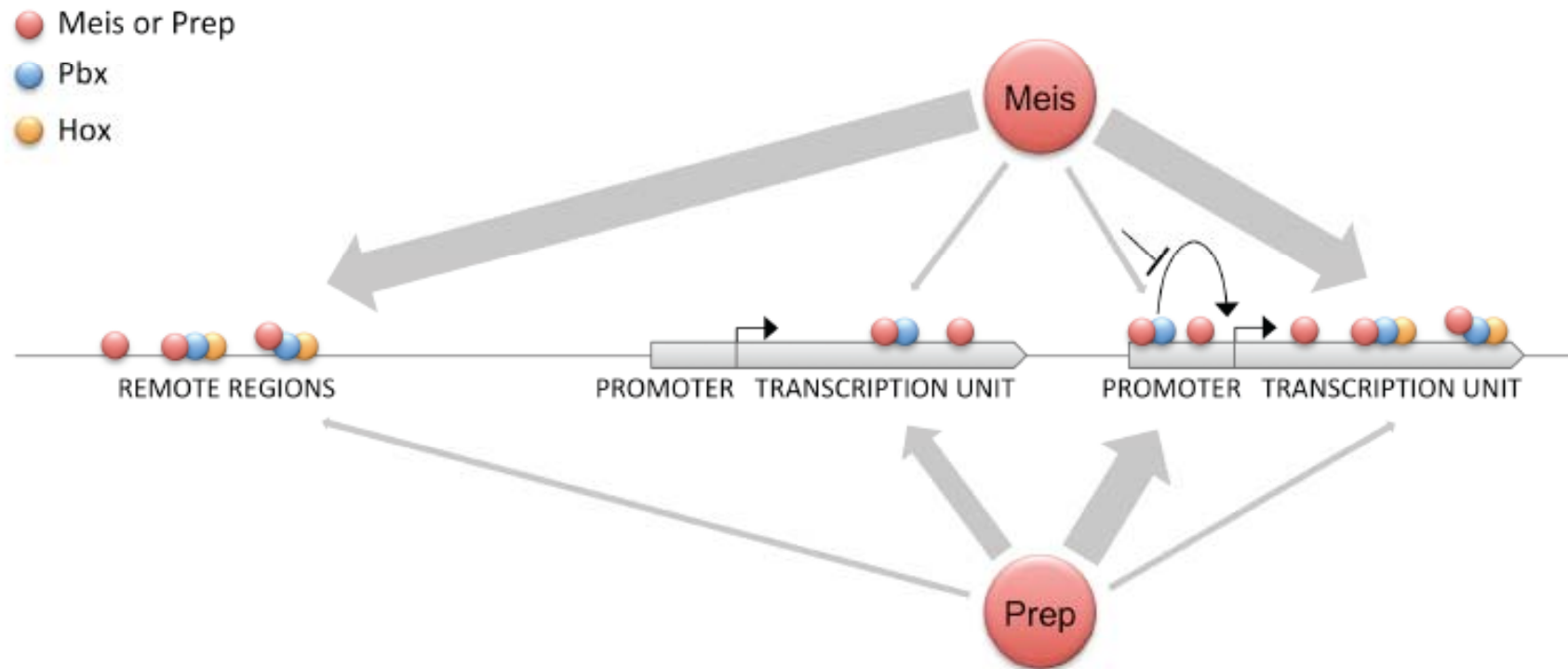


Figure 9. *P66<sup>Shc</sup> regulation of energetic substrate consumption and insulin-dependent gene expression in adipocytes.*

**A-B.** Cells were labeled with <sup>14</sup>C-oleate, left untreated or treated with insulin, as indicated. FA uptake and release were measured as <sup>14</sup>C incorporation (A) and <sup>14</sup>CO<sub>2</sub> release (B).

# Different mechanism of action of Prep1 and Meis1.



**Figure 10.** ChIPseq analysis shows that Prep1 and Meis1 have a different mechanism of action. Prep1 binds mostly at the start of the transcription units (genes), ie at promoters, whereas Meis1 binds either at remote regions or within transcription units but away from promoters. In addition, Prep1 and Meis1 can bind either in complex with Pbx and Hox proteins, or on Their own.